

Effect of Co-Flow Jet over an Airfoil: A Study on Flow Separation

¹Rakesh Kumar Rajak, ²Suryamani Kumar, ³Jyoti Tomar, Tannu Kumari
^{1,2,3} Department of Mechanical Engineering, Mumbai university, Thane, Maharashtra, India

ABSTRACT

Airfoil with co-flow jet (CFJ) has been a topic of interest among the researchers due to its important contribution in the various application like automobiles, commercial and military aircraft etc. CFJ is a technique to control the flow separation while fluid is flowing past the airfoil. The concept of CFJ airfoil is to open an injection slot near the leading edge from which a high-velocity jet is injected tangentially in the same direction of the main flow and allow the main flow to overcome adverse pressure gradient and the flow is remain attached by the help of a suction slot near the trailing edge which sucks the same amount of air that is injected from the injection slot. In the present study, Numerical analysis of NACA 2415 airfoil with co-flow jet (CFJ) is investigated using CFD package ANSYS fluent 16. Impact of the angle of attack and different free stream velocity on airfoil profile is studied.

Keywords: Airfoil Co-Flow jet (CFJ) Model, CFD, ANSYS FLUENT 16, Lift and Drag

1. INTRODUCTION TO CO-FLOW JET

1.1 Introduction

It has been noticed that fluid mechanics is used in most of problems in engineering field and flow over body is one of the widely studied problems. Flow over airplane will be major concerned in this study. When air flows over a body it causes two forces namely lift and drag. Lift and drag forces are main concern for evaluating the performance of airplane. When there is high speed flow over a solid body, an adverse pressure gradient along the flow start occurring which leads to boundary layer separation results in formation of wakes on the downstream. Wakes cause of reduction in the lift and increment in the drag force drastically. So the separation has been the main concerned in the aerodynamics.

Various works were done with aim to enhance the flow control and increase the lift, drag reduction and holding up the separation. Circulation control using tangential blowing technique at leading edge and trailing edge, a partial jolting technique on the upper surface are some of them. In this study, Numerical analysis is done on an NACA 2415 airfoil with co-flow jet technique. A long slot is prepared in airfoil nearly from leading edge to trailing edge on the low pressure surface in which a jet is allowed to go through the slot near to leading edge tangentially and the exact amount of mass flow is sucked away from the slot near to the trailing edge which creates a high turbulence and mixing between the main flow and jet, which raise the transverse movement of energy and allow the main flow to overcome the severe adverse pressure gradient and remain attached at high angle of attack. In case of CFJ airfoil, the mass flow rate in injection and suction is same results in the net energy expenses is reduced in comparison with the separation control by other techniques. In this method no moving parts are used results in less wear and maintenance is needed and easy to be followed.

1.2 Airfoil Theory

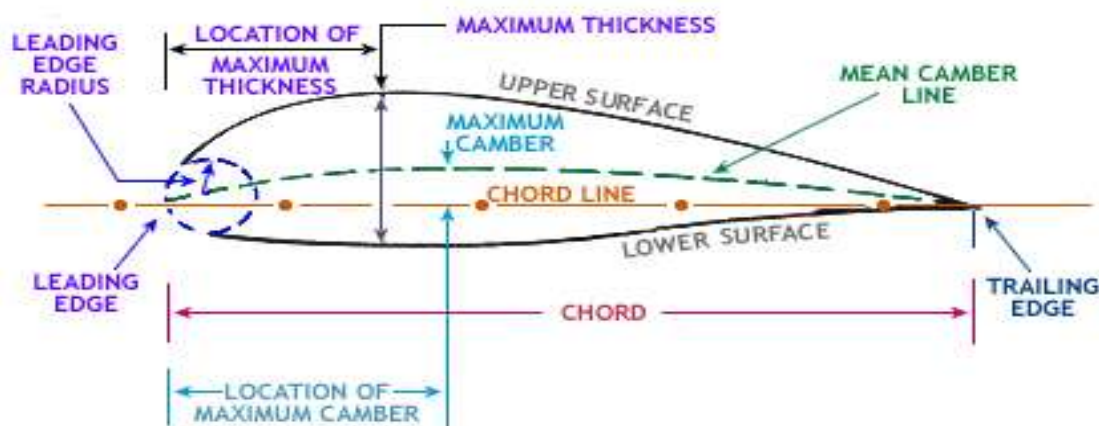


Fig. 1.1 Representation of airfoil section

1.3 The various terms in airfoils are described below:

- **Pressure surface** - is the lower side with comparatively higher pressure that is static pressure than the suction side.
- **Suction surface** - is the surface where there are higher velocity and low pressure.

1.4 The geometric terms related to airfoil is described below:

- **The trailing edge**- part of surface where there is a maximum curvature.
- **The leading edge**- the front point of airfoil where there is a maximum curvature.
- **Chord**- It is a length of the chord line. One of the features of the airfoil are specified in percentage of the chord measured from leading edge to trailing edge.
- **The chord line**- line joining the leading edge to the trailing edge and it is straight.

1.5 The parameters defining shape of an airfoil are:

- **The thickness** it varies from leading edge to the trailing edge so it is measured in two ways:
 - Perpendicular to the camber line
 - Perpendicular to the chord line.
- **Mean camber line (MCL)**: Line which is exactly in the middle of upper and lower surfaces is mean camber line. The MCL is above the chord line usually for a cambered airfoil whereas it coincides with the chord line for symmetric airfoils.
- **Maximum Thickness**- Maximum separation from the bottom edge to the top edge. It is usually 0.12c or 12% of the chord.
- **Maximum camber**. - Maximal distance in between the MCL and the chord line. Maximum Camber is usually specified as a % or fraction of the chord.
- **Leading Edge Radius**- The radius of curvature at the leading edge.
- **Stalling speed**: The slowest speed at which aircraft can fly in straight and level flight. It is defined in terms of the maximum lift coefficient as follows: -

$$L = \frac{1}{2} \rho V^2 SC_l \quad (1.1)$$

Where,

L= is the lifting force,

P= is the density of air,

V= is the relative velocity of the airflow,

S = is the area of the airfoil as viewed from an overhead perspective, and

CL is the lift coefficient.

Therefore, higher the lift, lesser the stalling speed.

Angle of attack is specified as the angle between the chord line and the relative wind direction or flight path.

Total aerodynamic force (TAF): The total force on the airfoil produced by the airfoil profile and relative wind.

Lift and Drag is the perpendicular component of TAF to the relative wind or flight path. **Drag** is the parallel component of TAF to the relative wind or flight path.

Flap: An artificial high lift providing device attached to the airfoil section at trailing edge. When flap is deflected downwards, the lift coefficient increases due to increase in camber of airfoil section.

2. GOVERNING EQUATIONS

2.1 Continuity Equation

$$\frac{\partial(\rho \bar{u})}{\partial x} + \frac{\partial(\rho \bar{v})}{\partial y} = 0 \quad (2.1)$$

2.2 Momentum Equation

Momentum equations in conservation form in x-direction is given by:

$$\frac{\partial(\rho \bar{u} \bar{u})}{\partial x} + \frac{\partial(\rho \bar{u} \bar{v})}{\partial y} = -\frac{\partial p}{\partial x} + \frac{\partial}{\partial x} \left(\lambda \nabla \cdot \vec{V} + 2\mu \frac{\partial u}{\partial x} \right) + \frac{\partial}{\partial y} \left[\mu \left(\frac{\partial \bar{v}}{\partial x} + \frac{\partial \bar{u}}{\partial y} \right) \right] + \rho B_x \quad (3.2)$$

Now, in y-direction given by:

$$\frac{\partial(\rho \bar{u} \bar{v})}{\partial x} + \frac{\partial(\rho \bar{v} \bar{v})}{\partial y} = -\frac{\partial p}{\partial y} + \frac{\partial}{\partial x} \left[\mu \left(\frac{\partial \bar{v}}{\partial x} + \frac{\partial \bar{u}}{\partial y} \right) \right] + \frac{\partial}{\partial y} \left(\lambda \nabla \cdot \vec{V} + 2\mu \frac{\partial v}{\partial y} \right) + \rho B_y \quad (3.3)$$

Equation 3.2 and 3.3 are completed Navier-stokes equation in conservation form, valid for steady and incompressible in 2-dimensional flow.

2.3 Energy equation

Now, energy conservation equation can be given:

$$\nabla \cdot \left[\rho \left(\mathbf{e} + \frac{v^2}{2} \right) \mathbf{V} \right] = \rho q + \frac{\partial}{\partial x} \left(k \frac{\partial T}{\partial x} \right) + \frac{\partial}{\partial y} \left(k \frac{\partial T}{\partial y} \right) - \frac{\partial (\rho \bar{u} p)}{\partial x} - \frac{\partial (\rho \bar{v} p)}{\partial y} + \frac{\partial}{\partial x} (\bar{u} \tau_{xx}) + \frac{\partial}{\partial y} (\bar{u} \tau_{yx}) + \frac{\partial}{\partial x} (\bar{v} \tau_{xy}) + \frac{\partial}{\partial y} (\bar{v} \tau_{yy}) + \rho B \cdot \vec{V} \quad (3.4)$$

In the equation where,

$$\vec{V} = \bar{u}\hat{i} + \bar{v}\hat{j}$$

From stokes relation,

$$\tau_{xx} = \lambda \nabla \cdot \vec{V} + 2\mu \frac{\partial \bar{u}}{\partial x} \quad (3.4b)$$

$$\tau_{yy} = \lambda \nabla \cdot \vec{V} + 2\mu \frac{\partial \bar{v}}{\partial y} \quad (3.4c)$$

$$\tau_{xy} = \tau_{yx} = \left(\mu \frac{\partial \bar{v}}{\partial x} + \frac{\partial \bar{u}}{\partial y} \right) \quad (3.4d)$$

3. DETAIL DESCRIPTION ABOUT CO-FLOW JET (CFJ)

There is various method are available for check the flow control techniques to augment the lift and keep the flow attached thereby increasing the stall margin of subsonic airfoils. So here Co Flow Jet (CFJ) is the one of the better techniques. In this method a jet is introduced through slots on the airfoil by using a pump and suction system. The main benefit of co-flow jet (CFJ) technique is that the increment in lift, high lifts at higher angle of attack, increasing stall margin and ultrahigh L/D ratios at cruise speeds. The other advantage is that unlike other flow control techniques which can be used only during landing and take-off this can be used during the entire duration of the flight.

No moving parts are required for this and hence the execution of the technique is quite so easy comparison to other circulation control techniques. This study was made to analyze the set-up of injection slot and suction slot and a comparison was made with the absence of suction slot. This paper proved that airfoils with different geometry gives different performance. It also proved that lower size of the injection slot gave better results than the same airfoil with twice the size of injection slot.

The effect of jet parameters on Co Flow Jet performance was studied by Ge-Cheng Zha et.al.[2]. Flow control via injection and suction slots were studied by T.L.Chng et.al[3]. The effect of injection slot size on performance of CFJ airfoil was studied by Ge-Cheng Zha et.al[4].

The CFJ model helps in reducing the takeoff and landing distances. It is easy to applied for both low and high speed aircrafts.

3.1 CFJ Model Details

Baseline airfoil is NACA2415

Model name – CFJ 2415-167-167, which is modification of the NACA2415 airfoil.

Table 3.1-Model dimension

Injection height	1.67% of chord length.
Suction height	1.67% of chord length.

Table 3.2-Location of slots.

Injection slots	6.72% of chord from the leading edge.
Suction slots	88.72% of chord from the leading edge.

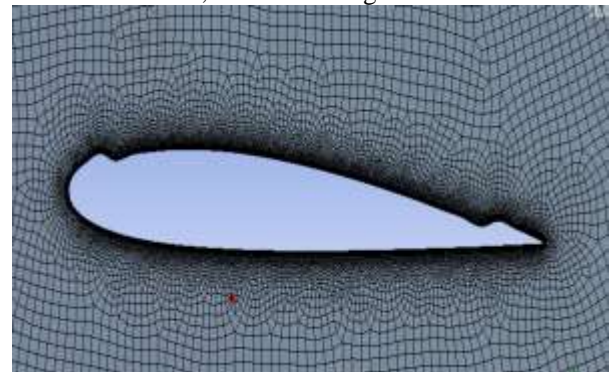
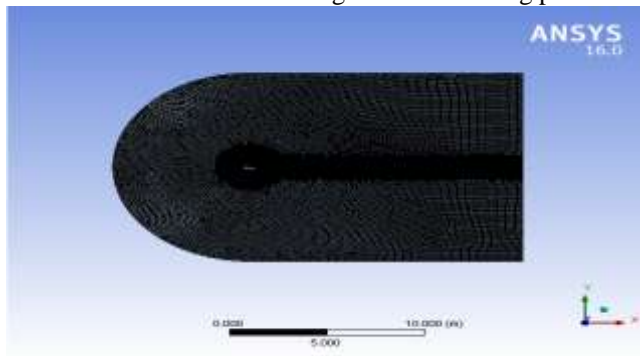
3.2 Operating and boundary condition

Table 3.3

No.	Input	Value
1	Velocity of flow	0.15 Mach or 51 m/s
2	Operating temperature	300 K
3	Operating pressure	101325 Pa.
4	Model	Transition
5	Density of fluid	1.225 Kg/m ³
6	Kinematic viscosity	1.4607 × 10 ⁻⁵
7	Reynolds number	3.5 × 10 ⁺⁶
8	Length	1m
9	AOA	4 degrees and 14 degree respectively
10	Fluid	Air as an ideal

3.3 Grid Topology

Grid topology has been chosen from literature survey, especially from Weatherill [8], who has described use of unstructured grid over multiply connected domains. He has particularly mentioned that, in order to capture the wall effect with unstructured grid. This meshing part has been done in ANSYS, as shown in figure: 4.2.3



4.2.3 - Meshing around CFJ 2415 Fig. 4.2.4 –

Closure view meshing.

3.4 Grid independence test

Grid independence test discussion in same way meshing work has been done from coarse, medium and fine steps. And result variation coefficient of lift (C_L) at $\alpha = 4^\circ$ is shown in below table:

Table: 4.4 Different value of C_L for varying element size

Sr No.	Element	Numerical Result (C_L)	Numerical Result (C_L) [8]	% error
1	15393	3.6638	4.0357143	9.203
2	24959	3.7803	4.0357143	6.329
3	70971	3.8748	4.0357143	3.987
4	140824	4.0609	4.0357143	0.624
5	276316	4.0553	4.0357143	0.4853
6	278824	4.0528	4.0357143	0.42336

3.5 Solver

The co-flow jet airfoil is simulated using CFD package ANSYS fluent 16. The governing equations are the 2D incompressible Navier-Stokes equations. A parabolic far-field boundary is used with the downstream boundary extended to 20 chord length and upstream to 15 chord length. The solver, the laminar boundary layer assumption is used. The freestream Mach number is 0.15 and the Reynolds number is 3.0×10^6 . Automatic method is used for structured mesh. In the injection slot the jet inlet hold a constant pressure equal to 1.315 times atmospheric pressure and in the suction slot the static pressure is iterated to match the jet inlet mass flow rate.

4. RESULTS AND DISCUSSIONS

4.1 Results of Co-flow jet (CFJ) airfoil

Here we have shown that in figure 4.1 the simulated data for $Re=3 \times 10^6$ for Co- flow and baseline aerofoil is compared. From this figure it is seen that the lift of the co- flow jet aerofoil increased dramatically with increased angle of attack and the stall angle is increased by 6° where the lift coefficient for co-flow jet airfoil is 2.677 which is 88.52% higher than the maximum lift coefficient for baseline aerofoil. As a result, the operating range of angle of attack is increased by 38.45%. The zero Lift angle of attack for co- flow jet aerofoil is around -6° and -2° for baseline airfoil.

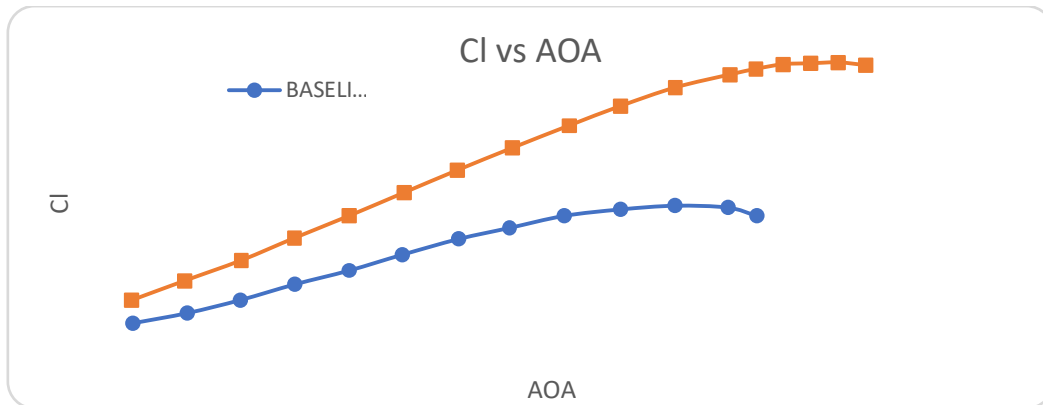


Figure 4.1 Lift coefficient vs AOA.

The Fig. 4.2 shows that streamlines at $AOA = 20^\circ$ in co-flow jet airfoil where the flow is smoothly attached to the aerofoil surface but the stall angle is 19° it is due to the fact that a strong vortex is developed adjacent to this layer which is shown from the velocity contour at $AOA = 20^\circ$ in fig 5.4. Where jet energy is mostly used to diffuse the flow to make the flow attached but the provided jet energy is not sufficient to diffuse this large wake hence the pressure drag is larger. In case of baseline aerofoil from fig.6.3 flow is separated even at 14° and a strong vortex is generated at the trailing edge of the aerofoil which dramatically reduces lift.

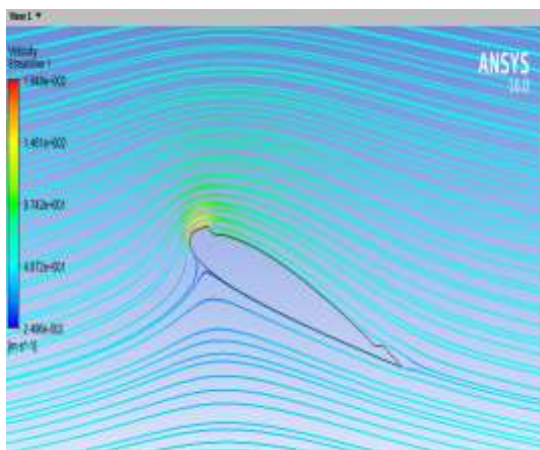


Fig. 5.2 Streamlines at AOA of 20° for co-flow jet airfoil.

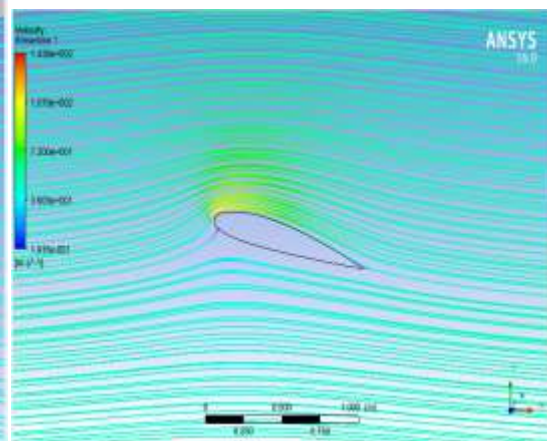


Fig. 5.3 Streamlines at AOA of 14° for baseline airfoil.

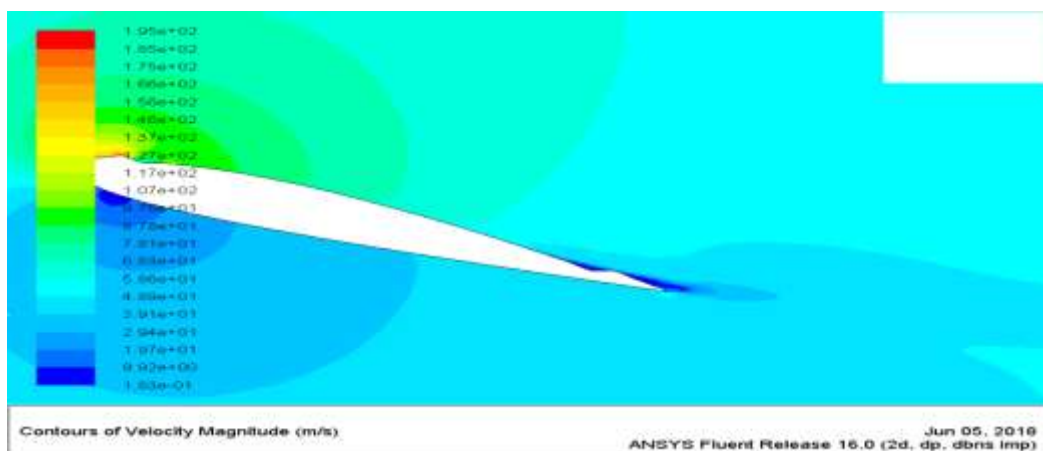


Figure 5.4 Velocity contour for Co-flow jet airfoil at $AOA = 20^\circ$

The drag of an airfoil is contributed from two sources, friction drag and pressure drag (form drag). The friction drag will always be in the opposite direction of the flight, that is, always positive. The negative drag hence must be from the pressure drag Fig.5.5 shows that the coefficient of drag for co-flow jet

airfoil is larger than baseline airfoil and it increases with increasing AOA. But from the fig. 5.6 it is seen that the Cl/Cd is much larger. This increased drag results from the turbulent mixing of jet and main flow. On basis of control volume analysis, the drag is determined by

When the AOA is very large the jet energy is not sufficient to fill the wake completely, only a part of wake is diffuse with main flow and remain attach with the airfoil, but the remaining wake produce large drag at high AOA. But as the cl/cd is large enough this high drag effect cannot much affect the cruising fight. From fig.5.6 it is also seen that the maximum Cl/Cd is obtained at the operating range of 4 to 6 degree for both baseline and co-flow jet airfoil. For this reason, the optimum operating range for normal flight is 4 to 6 degree.

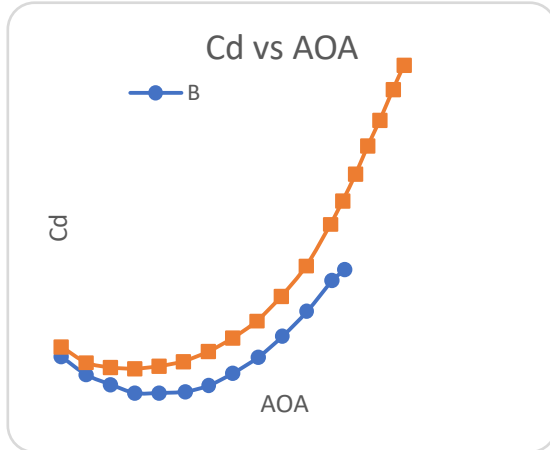


figure 5.5 Coefficient of drag vs AOA

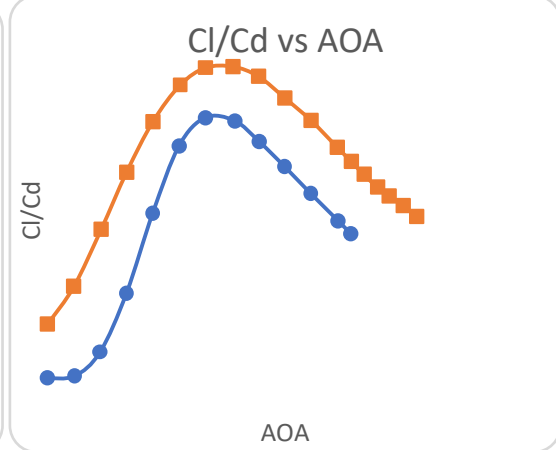


Figure 5.6 Cl / Cd Vs. AOA.

Fig. 5.7 indicates that the local maximum Mach number in the suction surface of the co-flow jet airfoil is supersonic and thus creates strong suction effect on the upper surface which is the reason for such high lift. the reason behind this high Mach number is that the high velocity jet will transfer the kinetic energy to the main flow through a low momentum wake. From fig. 5.9 it is seen that the negative pressure region in the upper surface of the co-flow jet airfoil is large. But in case of baseline airfoil from fig. 5.8 it is identified that the local Mach number is below the sonic value at 4 degree AOA and this subsonic airfoil is designed and operate in a manner that the maximum local Mach number on the surface of the airfoil must be less then sonic value otherwise it produces strong shock wave on the airfoil surface. Shock wave not generated in the co-flow jet airfoil because it energized the flow by injecting pressurized air.

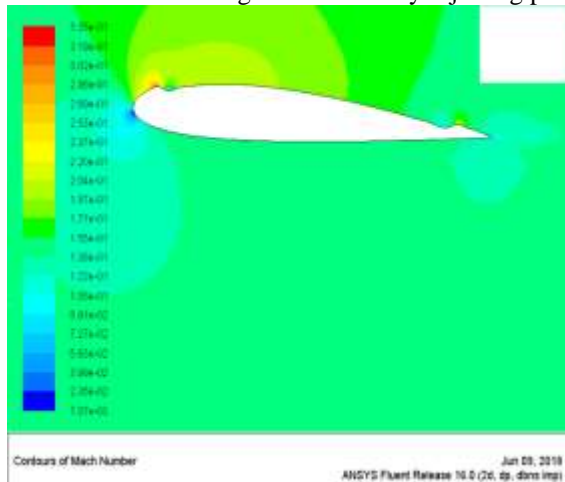


Fig.5.7: Mach number contours at AOA=4° for co-flow jet airfoil.

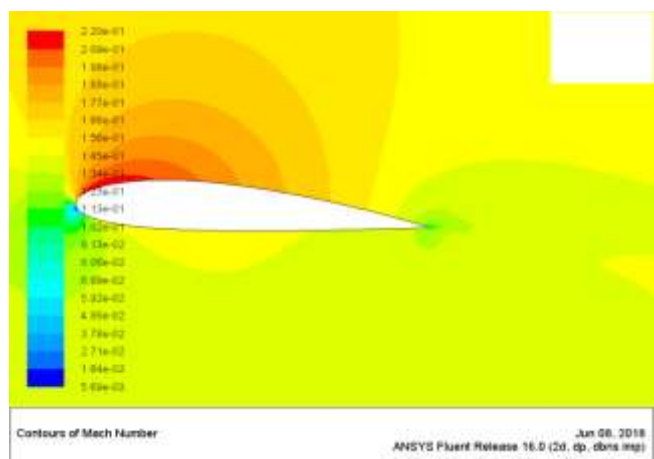


Fig.5.8: Mach number contours at AOA=4° for baseline airfoil

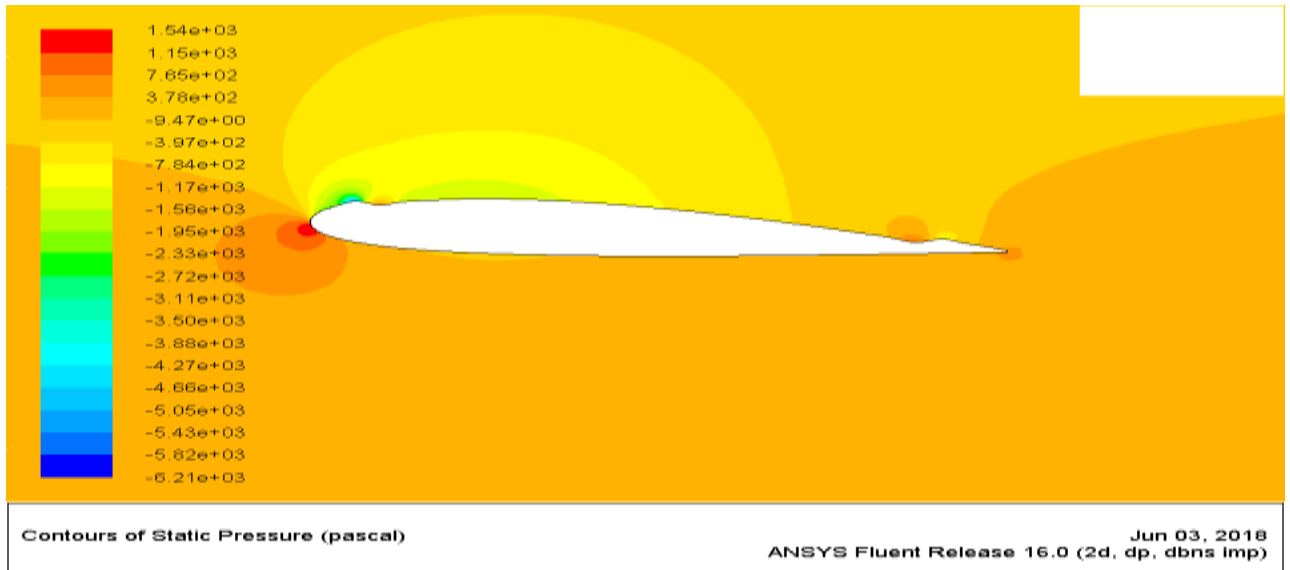


Fig.5.9: Pressure contours at AOA=4° for co-flow jet airfoil.

From fig.5.10 it is seen that for baseline airfoil wake start to generate even at 8-degree angle of attack. This wake starts to grow stronger with increasing angle of attack and separated the main flow from the airfoil surface. From fig.6.11, 6.12 and 6.13 it can be observed that at the trailing edge of the co-flow jet airfoil at AOA =10° no wake is formed but with increasing angle of attack wake is initiate to form at AOA=12° because the jet energy is not sufficient to fill the complete weak. The jet mixing only partially fills the wake which make the flow remain attached to the airfoil surface. But with increasing AOA the strength of the wake is also increased dramatically which cause the increasing drag at high AOA. After stall AOA attack such as at 20° it is observed that the flow is still remain attached to the airfoil (fig.5.2) but the lift decreased due to the presence of strong wake which produce adverse pressure gradient to the main flow and reduce the suction pressure on the suction surface of the airfoil. It may be possible to delay the formation of the wake on the airfoil suction surface by providing more energy to the jet which may energized the main flow and diffuse the wake. But in this case the energy expenditure may also increase. Experiment may be carried on to evaluate the optimum jet injection pressure for highest efficiency of the airfoil with minimum energy expenditure.

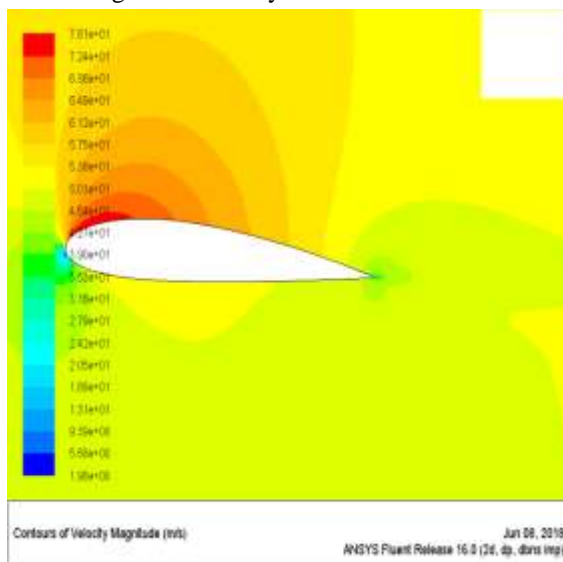


Fig.5.10: velocity contour at AOA= 4° for baseline airfoil.

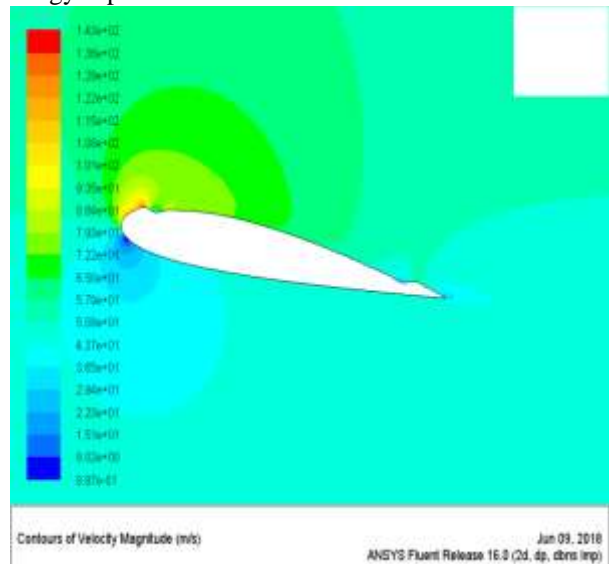


Fig.5.11: velocity contour at AOA=10° for co-flow jet airfoil.

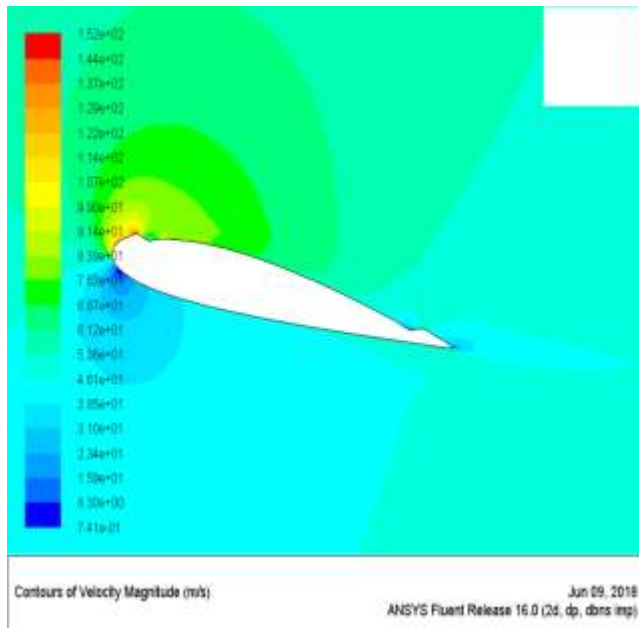


Fig. 5.12: velocity contour at AOA=12° for co-flow jet airfoil.

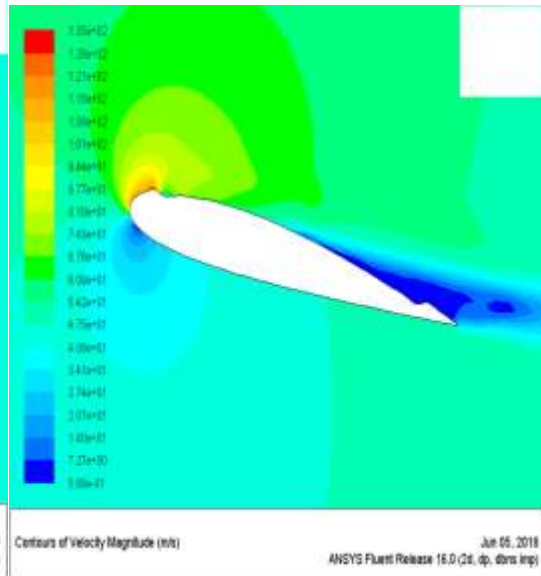


Fig.5.13: velocity contour at AOA= 14° for co-flow jet airfoil.

4.2 Parametric Results

4.2.1 Varying Deflection Angle of Angle

Table: 5.1 Variation of C_L and C_D with Angle of Angle of Baseline NACA2415

AOA in degree	Lift Coefficient	Drag Coefficient	Lift Force	Drag Force
0	$6.5157e^{+02}$	$2.3359e^{+01}$	240.63834	1.3059239
4	$1.7016e^{+03}$	$1.4198e^{+01}$	1042.2229	8.696456
10	$2.5314e^{+03}$	$3.6238e^{+01}$	2108.5452	23.6376
14	$4.3858e^{+03}$	$5.3709e^{+01}$	2686.2941	32.09671

Table: 5.2 Variation of C_L and C_D with Angle of Angle of CFJ NACA2415

AOA in degree	Lift Coefficient	Drag Coefficient	Lift Force	Drag Force
0	$2.4589e^{+03}$	$1.0241e^{+01}$	150.60805	6.2726931
4	$1.5765e^{+03}$	$1.45444e^{+01}$	965.59665	8.908102
6	$2.091e^{+03}$	$1.5373e^{+01}$	1285.6918	9.4159357
10	$3.1312e^{+03}$	$4.2319e^{+01}$	1917.8867	25.920289
12	$3.6318e^{+03}$	$6.4370e^{+01}$	2224.4751	39.426449
14	$2.8821e^{+03}$	$1.2341e^{+01}$	2603.2331	44.821551
20	$5.4396e^{+03}$	$8.7279e^{+01}$	3331.1074	53.406858

6. CONCLUSIONS AND FUTURE SCOPE

Airfoil with co-flow flow separation control technique is simulated using ANSYS fluent 16. It is observed that it provided a better performance than any other techniques in flow separation. A suction slot and injection slot are provided in upper side of airfoil with same mass flow rate. This technique can be easily applied due to no moving elements and other separation control method can be used with it to enhance it. It enhanced

lift force, delayed flow separation and attained dramatically high Cl/Cd. It significantly increases the Angle of Attack operating range and stall margin. In this process energy consumption is also low. Conclusively, it is capable to use in high and low speed aircraft.

Studies can be done on various other high lifting devices used by other aircrafts and comparative studies can be made. Turbulence model like DNS and LES can be used if super-computing facilities are available.

7. REFERENCES

- [1] Gias, M. T. I., Hossain, M. A., Hasan, M. M., & Mashud, M. Flow Separation Control on a NACA 0015 Airfoil using Co-Flow Jet (CFJ) Flow.
- [2] Prasad, K. S., & Vommi Krishna, B. B. Aerofoil Profile Analysis and Design Optimisation.
- [3] Zha, G. C., & Paxton, C. (2004, December). A novel airfoil circulation augment flow control method using co-flow jet. In *2nd AIAA Flow Control Conference* (p. 2208).
- [4] Zha, G. C., F Carroll, B., Paxton, C. D., Conley, C. A., & Wells, A. (2007). High-performance airfoil using coflow jet flow control. *AIAA journal*, 45(8), 2087-2090.
- [5] Abinav, R., Nair, N. R., Sravan, P., Kumar, P., & Nagaraja, S. R. (2016). CFD Analysis of Co Flow Jet Airfoil. *Indian Journal of Science and Technology*, 9(45).
- [6] Patel, K. S., Patel, S. B., Patel, U. B., & Ahuja, A. P. (2014). CFD Analysis of an Aerofoil. *International Journal of Engineering Research*, 3(3), 154-158.
- [7] Eleni, D. C., Athanasios, T. I., & Dionissios, M. P. (2012). Evaluation of the turbulence models for the simulation of the flow over a National Advisory Committee for Aeronautics (NACA) 0012 airfoil. *Journal of Mechanical Engineering Research*, 4(3), 100-111.
- [8] Xu, H., Xing, S., & Ye, Z. (2015). Numerical simulation of the effect of a co-flow jet on the wind turbine airfoil aerodynamic characteristics. *Procedia Engineering*, 126, 706-710.
- [9] Panigrahi, D. C., & Mishra, D. P. (2014). CFD simulations for the selection of an appropriate blade profile for improving energy efficiency in axial flow mine ventilation fans. *Journal of Sustainable Mining*, 13(1), 15-21.
- [10] Velazquez-Araque, L., & Nožička, J. (2014). Computational Analysis of the 2415-3S Airfoil Aerodynamic Performance. *Systemics, Cybernetics and Informatics*, 12(1).
- [11] Hoo, E., Do, K. D., & Pan, J. (2005). An investigation on the lift force of a wing pitching in dynamic stall for a comfort control vessel. *Journal of fluids and structures*, 21(8), 707-730.
- [12] Chng TL, Rachman A, Tsai HM, and Zha G-C. Flow control of an airfoil via injection and suction. *Journal of Aircraft*, 2009; 46(1):291–300.
- [13] Zha GC, Paxton CD, Conley CA, Wells A, Carroll BF. Effect of injection slot size on the performance of co flow jet airfoil. *Journal of Aircraft*, 2006; 43(4):987–95.
- [14] Zha GC, Carroll BF, Paxton CD, Conley CA, Wells A. High performance airfoil using co-flow jet flow control. *AIAA Journal*. 2007; 45(8):2087–90.
- [15] Zha GC, Paxton C, Gables C. A Novel Airfoil Circulation Augment Flow Control Method Using Co-Flow Jet. *2nd AIAA Flow Control Conference*. 2004. p. 1–13.